Journal of Alloys and Compounds 776 (2019) 242–249

Contents lists available at ScienceDirect

Journal of Alloys and Compounds

journal homepage: http://www.elsevier.com/locate/jalcom

Effect of intercritical annealing temperature on microstructure and mechanical properties of duplex Zr-2.5Nb alloy

Z.N. Yang [a, b, *], X.B. Wang [a], F. Liu [b], F.C. Zhang [a, b, **], L.J. Chai [c], R.S. Qiu [d], L.Y. Chen [e]

[a] State Key Laboratory of Metastable Materials Science and Technology, Yanshan University, Qinhuangdao, 066004, China
[b] National Engineering Research Center for Equipment and Technology of Cold Strip Rolling, Yanshan University, Qinhuangdao, 066004, China
[c] College of Materials Science and Engineering, Chongqing University of Technology, Chongqing, 400054, China
[d] College of Materials Science and Engineering, Chongqing University, Chongqing, 400044, China
[e] School of Science, Jiangsu University of Science and Technology, Zhenjiang, 212003, China

ARTICLE INFO

Article history:
Received 10 May 2018
Received in revised form
22 October 2018
Accepted 24 October 2018
Available online 25 October 2018

Keywords:
Zr-2.5Nb alloy
Annealing
Duplex microstructure
Mechanical property
Phase transformation

ABSTRACT

Duplex microstructure in Zr-Nb alloy possesses excellent mechanical properties. However, the effect of annealing temperature on the formation of duplex microstructure and its mechanical properties is not known. Determination of this effect is important for optimising the heat treatment process and expanding the knowledge of the microstructure. The detailed microstructure information and the relevant mechanical properties of the Zr-2.5Nb alloy annealed at 700 °C–900 °C have been studied. The amount of ω phase in alloy gradually increases and then decreases with increasing annealing temperature. The highest amount of ω phase is obtained in the specimen annealed at 750 °C, and no ω phase is formed when the specimen is annealed at 900 °C, which is mainly affected by the solution of Nb element in the β phase. The amount of primary α phase gradually decreases with increasing temperature, and its size remains stable at ~3 μm. However, the size of transformed β phase gradually increases from 1.5 μm to 12.4 μm. Mechanical property results reveal that the alloy annealed at 750 °C exhibits the highest strength of 996 MPa for the highest amount of ω phase, and the alloy annealed at 850 °C possesses the best ductility of 31.3%.

1. Introduction

Zr-2.5Nb alloy has been widely used in the chemical and nuclear industries due to their combined excellent irradiation stability and favourable corrosion resistance [1–5]. At room temperature, it comprises the major α phase and a small amount of β phase, and it possesses a hexagonal close-packed crystal structure (HCP) and a body-centred cubic structure (BCC), respectively. The transformation of β phase into α phase during the cooling process is notably influenced by the concentration of Nb element in it ($C_{Nb\text{-}\beta}$) at high temperature [6]. When the $C_{Nb\text{-}\beta}$ is lower than 6%, the α phase is formed during the cooling process, and when the $C_{Nb\text{-}\beta}$ is between 6% and 20%, ω phase is formed [7–9]. As $C_{Nb\text{-}\beta}$ further increases to 22%, the ω phase disappears, and a number of β phase is retained in room temperature [6]. This transformation process notably influences the mechanical properties of the alloy. The annealing treatment of the component, made of Zr-2.5Nb alloy after hot working procedure, is usually performed at an intercritical temperature within α+β phase region. The C_{Nb} in β phase gradually changes with increasing intercritical temperature, which influences the final microstructure and the relevant mechanical properties.

The newly developed duplex microstructure in Zr-Nb alloy is composed of primary α (α_p) and transformed β (β_T) phases (comprising secondary α [α_s] lamellae/acicular crystals in the continuous β matrix) via rolling deformation followed by a duplex-annealing treatment [10,11]. The duplex microstructure possesses not only excellent plasticity but also greater strength and toughness compared with the initial Widmanstätten microstructure. To obtain the duplex microstructure, the duplex-annealing treatment should be performed at an intercritical temperature to maintain a certain α_p phase. A temperature of 850 °C was the consistently used temperature [10–12]. For the conventional fabrication process of pressure tube, the intercritical annealing treatment is the optimal

* Corresponding author. State Key Laboratory of Metastable Materials Science and Technology, Yanshan University, Qinhuangdao, 066004, China.
** Corresponding author. State Key Laboratory of Metastable Materials Science and Technology, Yanshan University, Qinhuangdao, 066004, China.
E-mail addresses: zhinanyang@ysu.edu.cn (Z.N. Yang), zfc@ysu.edu.cn (F.C. Zhang).

https://doi.org/10.1016/j.jallcom.2018.10.320
0925-8388/

heat treatment after deformation process, which not only avoids the excessive growth of β phase and obtains the refined grain [13,14], but also guarantees high strength and high creep resistance for Zr-2.5Nb alloy [15]. Therefore, the duplex-annealing treatment for obtaining duplex microstructure in Zr-2.5Nb alloy is the most preferred option for making components, such as pressure tube. However, the effect of intercritical annealing temperature on the obtained microstructure and the relevant mechanical properties has not been investigated. This effect is important for optimising the heat treatment process of duplex microstructure in Zr-Nb alloy. Similarly, the duplex microstructure in Ti alloy has been widely studied [16,17]; it effectively improves the application of this kind of alloy.

In this paper, the Zr-2.5Nb alloy firstly underwent hot-rolled deformation prior to cold-rolling at room temperature. Finally, the alloy was annealed at various intercritical temperatures, followed by air cooling to room temperature. The final microstructure and mechanical properties have been studied in detail to reveal the effect of intercritical annealing on the microstructure and mechanical properties of the Zr-2.5Nb alloy.

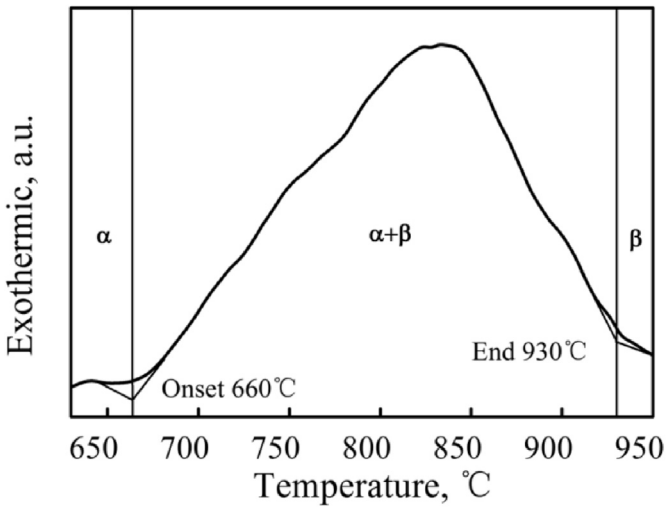

Fig. 1. DSC curve of received Zr–2.5%Nb alloy.

2. Experimental procedure

Typical Zr–2.5Nb alloy plates with the chemistry composition listed in Table 1 were used in this study. Differential scanning calorimetry (DSC) test shows that the initial transformation temperature of the alloy from α phase to β phase during the heating process is 660 °C, and the finishing transformation temperature is 930 °C, as shown in Fig. 1. The plates were subjected to the hot-rolling and cold-rolling deformation before annealing treatment, described as follows: the plates with dimensions of 100 mm × 40 mm × 10 mm (L × W × H) were firstly hot-rolled deformed at 850 °C with a reduction of ~50%, followed by air cooling to room temperature; then, the hot-rolled plates were rolled to a reduction of 50% at room temperature. Finally, these rolled plates were cut into pieces and annealed at an intercritical temperature of 700, 750, 800, 850 and 900 °C for 1 h, according to the phase map shown in Fig. 2a, followed by air cooling to room temperature.

Microstructural observations were performed by scanning electronic microscopy (SEM) and transmission electron microscopy (TEM). The specimens for SEM were firstly polished and then, etched using a mixture of 5 vol% hydrofluoric acid, 45 vol% nitric acid and 50 vol% distilled water. The specimens for TEM observation were thinned down to approximately 50 μm using SiC papers. Final thinning was achieved by electropolishing in an electrolyte mixture containing 10 vol% perchloric acid and 90 vol% methanol. The voltage was kept constant at 20 V, and the polishing was performed at −35 °C.

The XRD profile for each polished specimen was recorded by Rigaku D/max-2500 diffractometry using Cu-Kα radiation. The diffraction profiles were obtained by varying 2θ from 30° to 80° with a step scan of 0.02°. The time spent in collecting the data per step was 2 s. All specimens using tests were cut from the unannealed and annealed plates in the rolling direction. Vickers hardness measurements were performed on an FM-ARS 9000 hardness tester after the specimens were polished. A load of 200 g was applied for 10 s at each location. Dog-bone flat tensile specimens with a nominal gauge section of 5 mm × 3 mm × 2 mm (L × W × H), as shown in Fig. 2b, were cut from the unannealed and annealed plates in the rolling direction. Room temperature uniaxial tension tests were conducted using a Shimadzu AG-X Plus 10 kN with a strain rate of 1×10^{-3} s^{-1}. An extensometer was used to measure the strain change within the gauge section. All these experiments were performed at room temperature, and at least three specimens were used for each test to ensure the accuracy of result. The fracture surface morphologies of the failed specimens were examined using SEM to characterise the fracture mode of the alloy.

Table 1
Chemical composition of Zr-2.5Nb alloy (wt.%).

Nb	Fe	Ti	Hf	Other impurities	Zr
2.64	0.0043	0.0035	<0.010	<0.10	Balance

3. Results and discussions

3.1. Microstructural evolution

Fig. 3 shows the XRD patterns of the unannealed specimen and the specimens annealed at various intercritical temperatures. Two kinds of diffraction peaks are depicted in the unannealed specimen, representing α and β phases, respectively. When the annealing temperature is between 700 and 850 °C, another kind of diffraction peak representing ω phase can be detected. When increased to 900 °C, the ω phase disappears, and only α and β phases are left. As illustrated in Fig. 3, the peak intensity of ω phase is the highest for the specimen annealed at 750 °C, compared with that for other specimens, indicating that ω phase in that specimen has the most amount among the annealed specimens. During the annealing process, the amount of β phase at high temperature gradually increases with increasing intercritical temperature, as shown in Fig. 2a. However, the mean C_{Nb} in each phase decreases with increasing annealing temperature [18], which therefore, reduces the stability of β phase, and the amount of retained β phase after annealing treatment reduces with increasing annealing temperature, as shown in Fig. 3. For the unannealed specimen, which was air-cooled to room temperature after hot deformation process, more Nb atoms are retained in the α phase. These Nb atoms gradually diffuse into the neighbouring β phase during the annealing process, which inevitably increases the local C_{Nb} in β phase [19]. Moreover, the phase transformation from α phase to β phase occurs simultaneously, which inevitably results in the Nb atoms distributed heterogeneously in the β phase. Both the phase transformation rate and the diffusion rate of Nb element are notably increased with increasing temperature. The amount of β phase and the number density of lean Nb position determine the

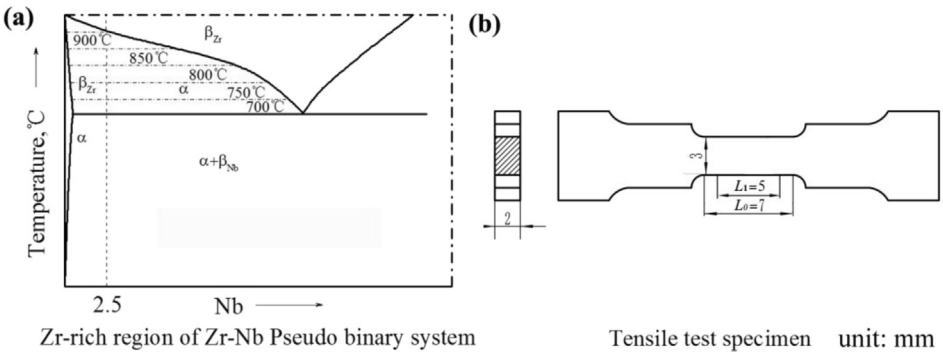

Fig. 2. Zr–rich region of Zr-Nb pseudo binary system (not to scale), showing annealing temperature in α+β phase field and its effect on α and β phase (a), and sketch of tensile specimen (b). Note: L_0 and L_1 in (b) represent the length of parallel section and gauge section, respectively.

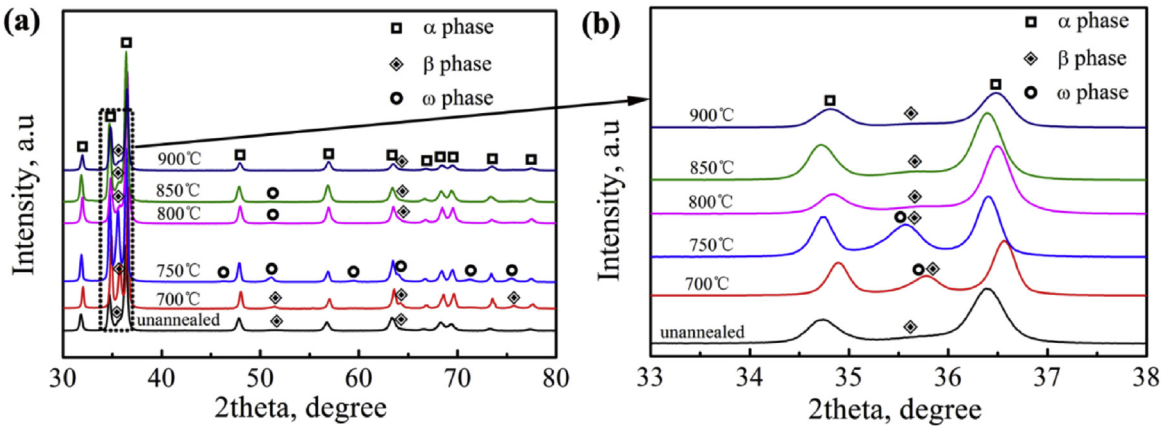

Fig. 3. XRD patterns of Zr-2.5Nb alloy annealed at various temperatures: integrated patterns (a) and partial patterns (b).

formation of ω phase during fast air cooling process, ~25 °C/s. Therefore, the distribution of Nb element in β phase is more heterogeneous at lower annealing temperature. Furthermore, during the cooling process, these places with lean Nb element in β phase are transformed into ω phase via athermal transformation [6–8,20]. Therefore, the amount of ω phase is highest in the specimen annealed at relatively lower temperature of 750 °C.

Fig. 4 shows the SEM micrographs of the unannealed specimen and the specimens annealed at various intercritical temperatures. The microstructure of the unannealed specimen consists of the elongated α phase and elongated transformed β phase due to the cold deformation, as shown in Fig. 4a. When the specimen is annealed at high temperature, static recrystallisation occurs during the holding process. For the specimen annealed at a temperature range of 700 °C–800 °C, the degree of recrystallisation gradually increases with increasing temperature, and the amount of equiaxed α and β phases gradually increases with increasing temperature, as shown in Fig. 4b–d. The observation showed on the top corner of Fig. 3b–d reveals that no α_s phase is formed within β phase during the air-cooling process, when the specimen is annealed at 700 and 750 °C. In addition, the β phase gradually transforms into α_s phase during the air-cooling process, when the annealing temperature reaches 800 °C. With further increase in annealing temperature, the amount of α_p phase gradually decreases along with an increased grain size of transformed β phase, as shown in Fig. 3e and f. The SEM observation is consistent with the XRD results, which show that the peak intensity of β phase is considerably higher for the specimen annealed at 700 °C and 750 °C, as compared with those annealed at high temperature. As mentioned above, during the annealing process, the C_{Nb} in β phase gradually decreases with increasing temperature, inevitably resulting in a gradually reduced stability of β phase with increasing temperature [18]. This event should be responsible for the increased number of β phase that can be retained into room temperature, when the deformed alloy is annealed at lower temperature of 700 °C and 750 °C.

The XRD results also reveal that there is ω phase in the specimen annealed at 700 °C and 750 °C. However, these ω particles cannot be directly observed via SEM for its small size. Fig. 5 shows the TEM observation for the unannealed specimen and the specimen annealed at various temperatures. A high density of dislocation within microstructure is noted, which provides the driving force for the recrystallisation process during the intercritical annealing process. Moreover, some dislocation cells can be observed in Fig. 5a, as indicated by the red arrows, indicating the dynamic recovery occurred during the cold-rolling deformation process for its high-stacking fault energy. This dynamic recovery phenomenon is similar to that obtained in a previous report on the tensile/compressive process of cold-rolled Zr-Nb alloy [21]. When the specimen is annealed at 700 °C, no dislocations can be seen in the α_p and β phases, and some β phases are located at the triple junction of α_p phase or between the α_p phases, as shown in Fig. 5b. A small amount of ω particles can also be detected within some β phases, as indicated by black arrows in Fig. 5b. Numerous ω particles can be observed within the β phase, when the specimen is annealed at 750 °C, as shown in Fig. 5c, which is consistent with the XRD result shown in Fig. 3. With increasing annealing temperature of 850 °C, α_s phase is distributed within β_T phase.

Fig. 6 shows the variation of volume fraction and the grain size

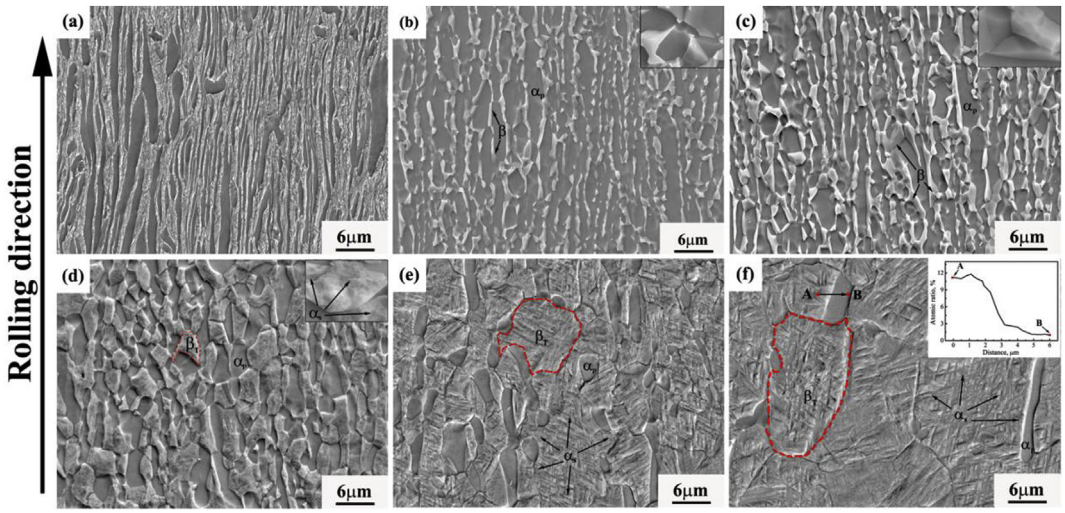

Fig. 4. SEM observations of Zr-2.5Nb alloy: unannealed specimen (a) and specimens annealed at 700 (b)、750 (c)、800 (d)、850 (e) and 900 °C (f). *Note:* the inset in the top right corner of (b)、(c)、(d) is a partly magnified version, and the inset in the top right corner of (f) is the variation of Nb content from positon A to B.

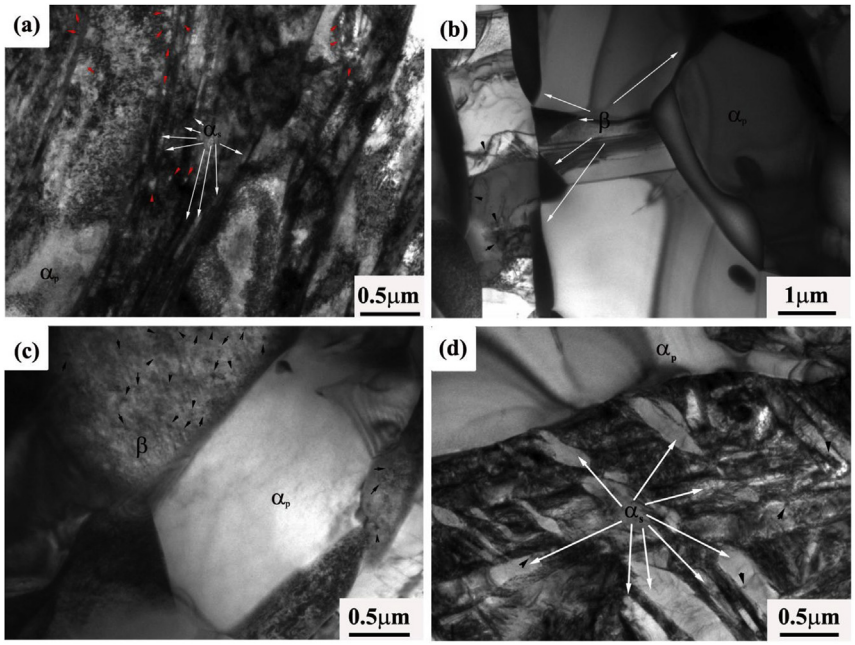

Fig. 5. TEM observations of Zr-2.5Nb alloy:unannealed specimen (a) and specimens annealed at 700 °C (b),750 °C (c) and 850 °C (d). *Note:* black arrows indicate ω particles.

of α_p phase, and β_T phase with increasing annealing temperature. The morphologies of α_p and β_T phases are still extended, when the specimen is annealed at 700 °C. Therefore, the grain size of the two phases is not concluded in Fig. 6b. As shown in Fig. 6a, from 700 °C to 900 °C, the volume fraction of α_p phase gradually decreases from 72.90% to 8.16%; a slightly higher decrease rate is noted when it is lower than 750 °C. The grain size of α_p phase is nearly unchanged and maintained at ~3 μm, when at 750–900 °C, which is similar to that observed before on the Zr-Nb alloy annealed at 850 °C for different time [10]. During the annealing process, the static recrystallisation process of each phase and the transformation from α phase to β phase start simultaneously. This event probably results in that the growth of recrystallised α grain is counteracted by the phase transformation process. Moreover, the initial size of α phase before hot deformation process can also influence the final grain size of α phase [22]. However, with increasing annealing temperature from 750 °C to 900 °C, the grain size of β_T phase directly increases from ~1.54 μm to ~12.41 μm, with a considerably higher growth rate after 850 °C. This observation mainly results from the faster phase transformation rate at higher temperature. The annealing temperature of 900 °C is higher than the hot deformation temperature, providing a higher driving force for β phase growth. Moreover, the migration rate of the grain boundary increases at higher temperature. This results from the decreasing $C_{Nb\text{-}\beta}$ value with increasing temperature, thereby reducing the inhibition effect of alloying element on grain diffusion [11].

3.2. Mechanical properties

Fig. 7 shows variation in average hardness of the specimen with

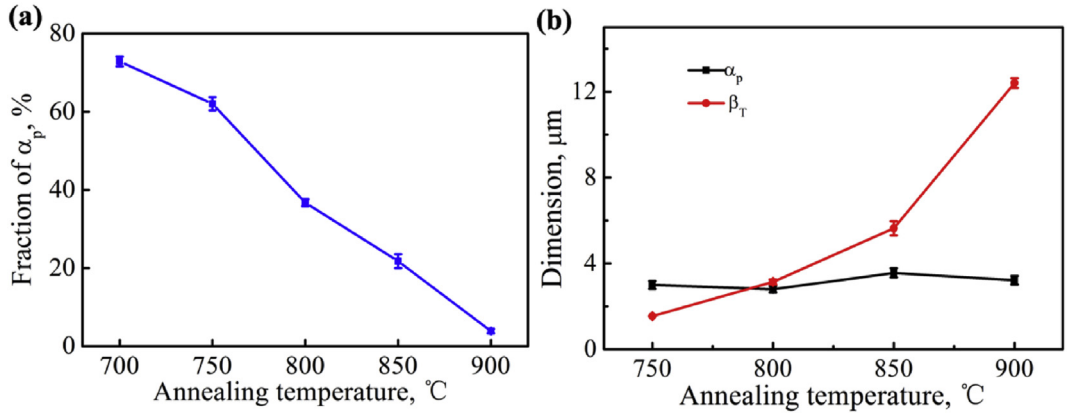

Fig. 6. Variation of volume fraction of α_p phase (a) and the grain size of α_p phase and β_T phase (b) with increasing annealing temperature.

increasing annealing temperature. The initial hardness of the specimen is 260 HV, which increases after being annealed at high temperature. The hardness of the hot-rolled specimen firstly increases from 260 HV to 293 HV (the highest value) at 750 °C, and then, decreased monotonously to 263 HV at 850 °C. Finally, the hardness slightly increases to 273 HV at 900 °C. The numerous precipitated ω particles in the microstructure should be responsible for the highest hardness of specimen annealed at 750 °C, although a relatively higher content of soft β phase is observed. Moreover, the solution-strengthening effect of Nb element in α and β phases is higher at lower temperature than that at higher temperature due to the decreased C_{Nb} in both phases with increasing intercritical annealing temperature. This phenomenon is similar to that occurred during the aging process of the Zr-Nb alloy at low temperature of 300 °C–500 °C [23,24], according to Fig. 2a. At 900 °C, only 5% of α_p phase left, and the α_s phase becomes the major phase, as shown in Fig. 4. The C_{Nb} in α_s phase is higher than that in α_p phase [11], resulting in a higher solution-strengthening effect. Combining the strengthening effect from refined grain size, the hardness of α_s phase should be higher than that of α_p phase. Therefore, the hardness of the annealed specimen exhibits a slight increment after being annealed at 900 °C.

Fig. 8 shows the engineering stress-strain curves of the unannealed specimen and the specimen annealed at various temperatures, with the detailed mechanical properties being summarised in Table 2. When the specimen is annealed at 700 °C, the yield strength is reduced from the initial 815 MPa–765 MPa, and the tensile strength is nearly unchanged, as compared with the unannealed specimen. At 750 °C, the yield strength and the tensile strength increase to 842 MPa–996 MPa, respectively. With further increasing temperature to 900 °C, the yield strength monotonously decreases to 643 MPa, and the tensile strength gradually decreases to 876 MPa for the 850 °C specimen, with a slight increase to 896 MPa for the 900 °C specimen. The elongation evolution is adverse to the strength. The variation in strength of the alloy is determined by the microstructure evolution. As shown in Fig. 5a, a high density of dislocation interior of the microstructure is noted, which contributes to the high strength of the unannealed specimen. After the annealing process of the cold-rolled specimen, the dislocation density notably decreases, as shown in Fig. 5b–d. Moreover, for the specimen annealed at 700 °C, a higher amount of β phase is retained at room temperature. These two factors lower the yield strength and the tensile strength, and increase the ductility of the alloy. However, ω particles are precipitated during the cooling process, which has a characteristic of hard and brittle [8], contributing to the tensile strength of the alloy. A small amount of ω phase is precipitated in the microstructure of the specimen annealed at 700 °C, which offsets a certain weakened effect on strength from the decreased dislocations and β phase, and results in a nearly unchanged tensile strength. Some studies also revealed that a small amount of ω phase has a negligible effect on ductility [8,9]. Therefore, the specimen annealed at 700 °C also shows an increased ductility, as compared with unannealed condition. For

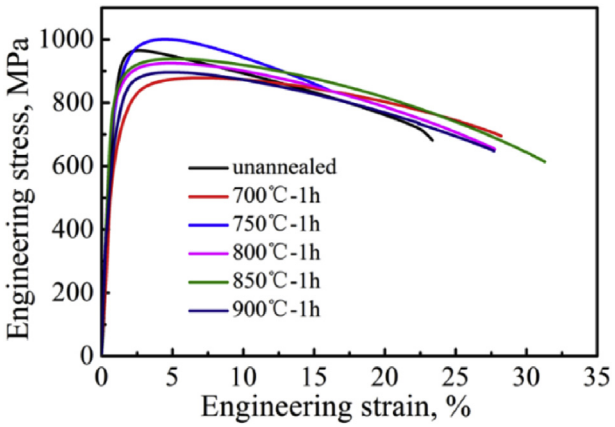

Fig. 8. Engineering stress-strain curves of the Zr-2.5Nb alloy annealed at various temperatures.

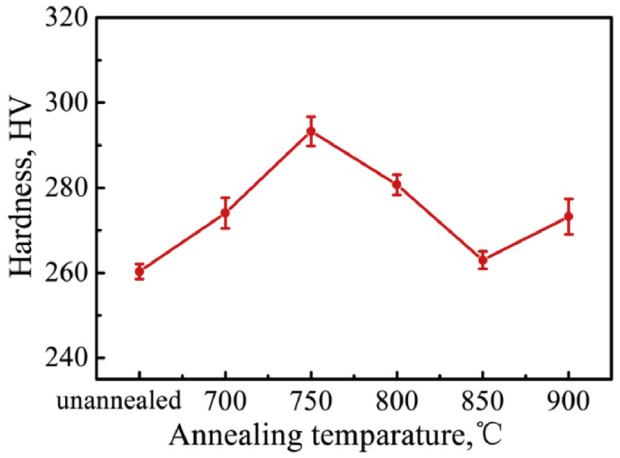

Fig. 7. Variation in average hardness of Zr-2.5Nb alloy with increasing annealing temperatures.

Table 2
Mechanical properties of Zr-2.5Nb alloy after annealing at various temperatures.

Annealing temperature/°C	Hardness/HV	$\sigma_{0.2}$/MPa	σ_b/MPa	δ/%	δ_{gt}/%	$\sigma_b \times \delta$/GPa·%
unannealing	260 ± 2	815 ± 7	978 ± 8	23.7 ± 1.9	2.2 ± 0.6	23.2 ± 0.8
700	274 ± 4	765 ± 5	976 ± 6	27.2 ± 1.1	6.2 ± 0.9	26.5 ± 0.5
750	293 ± 5	842 ± 10	996 ± 6	15.2 ± 0.1	3.6 ± 0.6	15.1 ± 0.2
800	281 ± 3	770 ± 4	940 ± 15	27.2 ± 0.2	4.2 ± 0.3	25.6 ± 0.4
850	263 ± 2	738 ± 9	876 ± 11	31.3 ± 0.7	5.0 ± 0.4	27.4 ± 0.7
900	273 ± 4	643 ± 13	896 ± 6	27.2 ± 1.1	4.8 ± 0.1	24.4 ± 0.5

the alloy annealed at 750 °C, numerous ω particles are precipitated in the β phase, which not only notably increases the strength but also deteriorates the ductility of the specimen. When the annealing temperature is further increased to 850 °C, the amount of ω particle is notably decreased, and eventually disappeared, which should be responsible for the increased elongation. When the alloy is annealed at 900 °C, the microstructure become coarsen, and the amount of retained soft β is decreased, resulting in a slightly decreased elongation as compared with the specimen annealed at 850 °C. According to the static toughness values, which are estimated via strength and elongation, the specimen annealed at 850 °C possesses the best comprehensive mechanical properties.

It also should be noted that the uniform elongation of the alloy is relatively low and is nearly the same for all annealed specimens, as shown in Table 2. Previous study on the cold-deformed Zr-Nb alloy has revealed that dynamic recovery should be responsible for the strain-softening behaviour occurred during the tensile and compressive processes [21]. However, the present alloy is conditioned under hot deformation with cold deformation, followed by annealing at intercritical temperature. The dislocation density interior of the microstructure should be considerably lower than the cold deformation condition, and few dislocations are prepared for the occurrence of dynamic recovery during the initial tensile process, as shown in Fig. 5b–d. Therefore, the low-uniform elongation on the present study should be different from that reported in Ref. 26. Fig. 9 shows the hardness evolution of some tensile specimens from the site near the fracture surface to the site within the uniform deformation region. The hardness in the necking region is higher than that in the uniform deformation region. The hardness in the uniform deformation region is nearly the same, thereby indicating that the deformation is homogeneous before necking. The hardness in the necking region gradually increases with closing to the fracture surface, which reveals a gradually strain-hardening behaviour of the unannealed and annealed alloys during the tensile process. This event also indicates that the conventional partial plastic instability should be responsible for the occurrence of necking.

The cross-section tensile fractographs of the unannealed specimen and the specimens annealed at 700, 750 and 850 °C, shown in Fig. 10, reveal a typical ductile fracture mode for all specimens. The mechanism of ductile fracture consists of three distinct stages: void nucleation in the first state, void growth in the second state, and then, void coalescence and eventual fracture [25,26]. For the specimen annealed at 700 and 750 °C, the duplex microstructure has not been formed, and there are more ω particles within the β phase, especially for the 750 °C specimen. More hard and brittle ω particles facilitate the void nucleation at the interface of ω phase and β phase. And for duplex microstructure in Zr-2.5Nb alloy, previous study has revealed that the nucleation sites of microvoids were mainly on the interfaces of α_p and β_T phases [11], due to the incompatibilities of local stress and strain on the globular and lamellar colony. Moreover, the impurity elements, such as Fe, Cr and Ni, are prone to gather at the interface, occurring during the annealing process and then, weakening the strength of the interface [27]. In the present study, numerous interfaces of α_p and β_T phases are observed, which may be responsible for the low uniform elongation. The method that can improve the uniform ductility of duplex microstructure should be further studied.

Moreover, from the low magnification observations shown in the top right corner of fractographs in Fig. 10, it can be seen that the fracture surface seems to more flat and the depth of dimple is smaller for the unannealed specimen than those for annealed specimens. It also can be seen that there are more secondary cracks in the 750 °C specimen as compared with others, indicating a relatively lower ductility.

4. Conclusion

In this paper, the detailed microstructure evolution and mechanical properties of the cold-rolled Zr-2.5Nb alloy after intercritical annealing treatment have been studied. The following results were obtained:

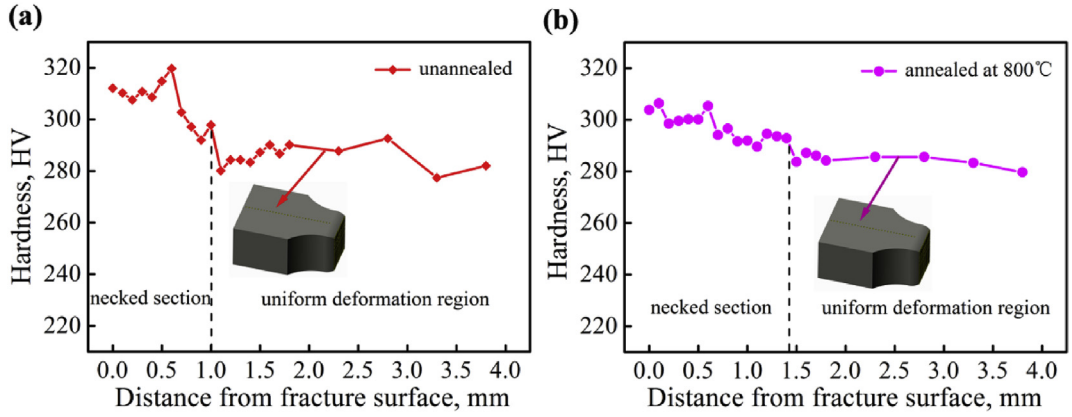

Fig. 9. Variation in hardness for the failure specimen with increasing distance from the fracture surface.

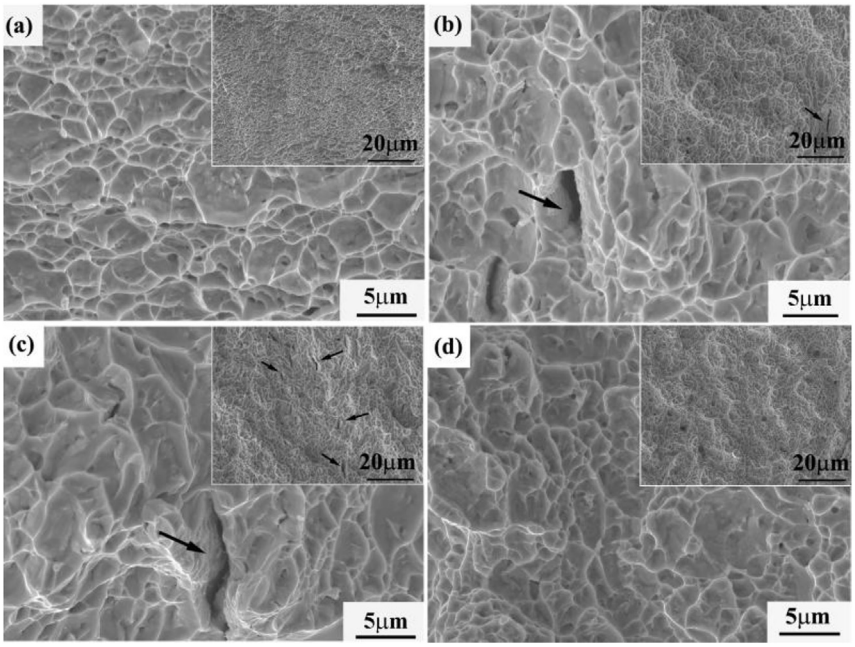

Fig. 10. Cross-section fractographies of Zr-2.5Nb alloy: unannealed specimen (a) and specimen annealed at 700 °C (b) and 750 °C (c) and 850 °C (d). Note: the insets in the top right corner are low magnification versions of the fractographies, and the black arrow in (b) and (c) are secondary cracks.

1) When the intercritical annealing temperature is below 800 °C, the duplex microstructure does not form, with a polygonal α and β phase being retained at room temperature. In addition, the amount of ω phase, precipitated during the air-cooling process, is highest in the specimen annealed at 750 °C due to the highest amount of β phase and the relatively lower C_{Nb}.
2) The duplex microstructure is formed when the annealing temperature reaches 800 °C, and a certain amount of ω phase is formed, except for the specimen annealed at 900 °C. The size of α_p phase is nearly unchanged and maintains at ~3 μm, and the grain size of β_T phase directly increases from ~1.54 μm to ~12.41 μm at 900 °C.
3) The specimen annealed at 750 °C possesses the highest hardness and strength, as compared with other specimens, due to the large amount of ω particles. In addition, the specimen annealed at 850 °C shows the lowest strength but the highest ductility, which presents the highest static toughness, as compared with the other specimens.
4) The uniform elongation of the annealed alloy is relatively low (~3.6%–6.2%), which is mainly due to the incompatibilities of local stress and strain on the α_p and β_T phases during the tensile deformation process. This event is the weakness of duplex microstructure in Zr-2.5Nb alloy, and the method used to improve its uniform ductility should be further studied.

Acknowledgements

This work was supported by the National Natural Science Foundation of China (No. 51601165, 51401040, 51501021, 51601075) and the Natural Science Foundation of Hebei Province of China (E2015203250).

References

[1] F. Long, L. Balogh, D.W. Brown, et al., Effect of neutron irradiation on deformation mechanisms operating during tensile testing of Zr-2.5Nb, Acta Mater. 102 (2016) 352–363.
[2] H.L. Yang, Y. Matsukawa, S. Kano, et al., Investigation on microstructural evolution and hardening mechanism in dilute Zr–Nb binary alloys 481 (2016) 117–124.
[3] L.J. Chai, S.Y. Wang, B.F. Luan, et al., Electron backscatter diffraction investigation of duplex-phase microstructure in a forged Zr-2.5Nb alloy, Sci. China 59 (4) (2016) 673–679.
[4] C. Silva, K. Leonard, M. Trammel, et al., Characterization of different forms of Zr-2.5Nb samples before and after neutron irradiation, Mater. Sci. Eng. A 716 (2018) 296–307.
[5] S.J. Zinklea, G.S. Was, Materials challenges in nuclear energy, Acta Mater. 61 (3) (2013) 735–758.
[6] R. Kondo, N. Nomura, Suyalatu, et al., Microstructure and mechanical properties of as-cast Zr-Nb alloys, Acta Biomater. 7 (2011) 4278–4284.
[7] M. Todai, K. Fukunaga, T. Nakano, ω phase transformation and mechanical properties in binary Zr-Nb biomedical alloy, Mater. Sci. Forum 879 (2016) 1969–1973.
[8] J.C. Williams, D.De Fontaine, N.E. Paton, The ω-phase as an example of an unusual shear transformation, Metall. Trans. 4 (1973) 2701–2708.
[9] J. Šmilauerová, P. Harcuba, J. Pospíšil, et al., Growth of ω, inclusions in Ti alloys: an X-ray diffraction study, Acta Mater. 61 (17) (2013) 6635–6645.
[10] Z.N. Yang, F.C. Zhang, F.C. Liu, et al., Achieving high strength and toughness in a Zr–2.3Nb alloy by the formation of duplex microstructure, Mater. Des. 40 (2012) 400–406.
[11] Z.N. Yang, F.C. Zhang, L. Qu, et al., Formation of duplex microstructure in Zr-2.3Nb alloy and its plastic behaviour at various strain rates, Int. J. Plast. 54 (2) (2014) 163–177.
[12] M. Zhang, F.C. Zhang, Z.N. Yang, et al., Effect of cooling process on the formation of duplex microstructure in Zr-2.3Nb alloy, J. Alloys Compd. 651 (2015) 316–321.
[13] R. Kapoor, J.K. Chakravartty, C.C. Gupta, et al., Characterization of superplastic behaviour in the (α+β) phase field of Zr-2.5 wt.% Nb alloy, Mater. Sci. Eng. A 392 (1–2) (2005) 191–202.
[14] D. Lee, W.A. Backofen, Superplasticity in some titanium and zirconium alloys, Trans. Metall. Soc. AIME 239 (7) (1967) 1034–1040.
[15] R.V. Kulkarni, K.V.M. Krishna, S. Neogy, et al., Mechanical properties of Zr–2.5%Nb pressure tube material subjected to heat treatments in α+β phase field, J. Nucl. Mater. 451 (1–3) (2014) 300–312.
[16] S.K. Jha, C.J. Szczepanski, R. John, et al., Deformation heterogeneities and their role in life-limiting fatigue failures in a two-phase titanium alloy, Acta Mater. 82 (2015) 378–395.
[17] K. Wang, M. Wu, Z. Yan, et al., Dynamic restoration and deformation heterogeneity during hot deformation of a duplex-structure TC21 titanium alloy, Mater. Sci. Eng. A 712 (2017) 440–452.
[18] H. Okamoto, Alloy Phase Diagrams. ASM Hand Book, vol. 3, ASM International, 1992.
[19] M. Zhang, Y.N. Li, F.C. Zhang, et al., Effect of annealing treatment on the microstructure and mechanical properties of a duplex Zr-2.5 Nb alloy, Mater. Sci. Eng. A 706 (2017) 236–241.
[20] G. Lutjering, Influence of processing on microstructure and mechanical properties of (α+β) titanium alloys, Mater. Sci. Eng. A 243 (1998) 32–45.

[21] Z.N. Yang, F.C. Zhang, Y.Y. Xiao, et al., Dynamic recovery: the explanation for strain-softening behaviour in Zr-2.3Nb alloy, Scripta Mater. 67 (12) (2012) 959–962.
[22] X.D. Wu, G.J. Yang, P. Ge, et al., Induction of β-titanium alloy and its solid state transition, Titan. Ind. Prog. 25 (5) (2008) 1–6.
[23] V.D. Hiwarkar, S.K. Sahoo, I. Samajdar, et al., Annealing of cold worked two-phase Zr-2.5Nb-Associated microstructural developments, J. Nucl. Mater. 384 (2009) 30–37.
[24] R. Kishore, R.N. Singh, G.K. Dey, et al., Age hardening of cold-worked Zr-2.5 wt % Nb pressure tube alloy, J. Nucl. Mater. 187 (1992) 70–73.
[25] S.M. Keralavarma, S. Chockalingam, A criterion for void coalescence in anisotropic ductile materials, Int. J. Plast. 82 (2016) 159–176.
[26] M.J. Nemcko, J. Li, D.S. Wilkinson, Effects of void band orientation and crystallographic anisotropy on void growth and coalescence, J. Mech. Phys. Solids 95 (2016) 270–283.
[27] V. Perovic, A. Perovic, G.C. Weatherly, et al., Microstructural and microchemical studies of Zr-2.5Nb pressure tube alloy, J. Nucl. Mater. 205 (1) (1993) 251–257.